Int. J. Anal. Appl. (2025), 23:197

International Journal of Analysis and Applications

Application of Cryptography for Controllability Results of Fractional Neutral Volterra-Fredholm Integro-Differential Equations with State-Dependent Delay

Prabakaran Raghavendran[1,*], Tharmalingam Gunasekar[1,2], Ahmad Aloqaily[3], Nabil Mlaiki[3]

[1] *Department of Mathematics, Vel Tech Rangarajan Dr.Sagunthala R&D Institute of Science and Technology, Chennai - 600062, Tamil Nadu, India*

[2] *Department of Mathematics, Institute of Engineering and Technology, Srinivas University, Mukka, Mangaluru, Karnataka 574146, India*

[3] *Department of Mathematics and Sciences, Prince Sultan University, 11586 Riyadh, Saudi Arabia*

[*] *Corresponding author:* rockypraba55@gmail.com

Abstract. This paper utilizes the Caputo fractional derivative and a semigroup of compact and analytic operators to examine the controllability of fractional Volterra-Fredholm integro-differential equations with state-dependent delay. Controllability results are formulated using Schauder's fixed point theorem, addressing the inherent difficulties brought about by the fractional dynamics together with state-dependent delays. The theoretical findings are validated through a detailed example and numerical simulations, demonstrating the convergence of solutions. Graphical representations are provided to better understand solution dynamics and highlight system complexity. Additionally, the applicability of the proposed system for cryptographic key generation is explored, showing that it can generate secure, unpredictable keys due to its chaotic behavior, sensitivity to initial conditions, and the interplay between key system parameters.

1. Introduction

The fractional Volterra-Fredholm integro-differential equations (VFIDEs) with a state-dependent delay (SDD) have become highly prominent in study due to the wide range of applications in natural sciences and engineering [1–3]. This class of equations is characterized by the fractional derivative, which better models the nature of these memory-sensitive and hereditary systems. A crucial source to study fractional differential equations is the work by Zhou, which introduces readers to a deep insight of the fundamental theory of the said equations along with key ideas and mathematical representations [4]. Extensive works done by Kilbas, Srivastava, and Trujillo elaborate more on the theory and application of such differential equations that can be used as the

Received: Mar. 13, 2025.

2020 *Mathematics Subject Classification.* 34A08, 45J05, 65L20, 93C23, 68T07.

Key words and phrases. Caputo fractional derivative; Schauder fixed point theorem; numerical simulations.

https://doi.org/10.28924/2291-8639-23-2025-197

ISSN: 2291-8639

cornerstone of study of fractional calculus [5]. In fractional integro-differential equations with SDD, Agarwal and Andrade explain the different challenges that this system of equations provides. Their contribution highlights the intricacy of modeling systems where the future behavior is dependent on the current state as well as the previous states [6]. Similarly, Benchohra and Berhoun's work further expands this knowledge by investigating impulsive fractional differential equations with SDD, which contributes much to the study of dynamic systems with sudden jumps and memory [7]. Guendouzi and Bousmaha's work on the approximate controllability of fractional neutral stochastic functional integro-differential inclusions with infinite delay shows that controllability is crucial in fractional systems, especially in uncertain systems and time-delayed systems [8]. Liu and Bin's work on impulsive Riemann-Liouville fractional differential inclusions provides an essential perspective on how impulsive effects interact with fractional dynamics, adding complexity to the solution methods [9].

Balasubramaniam and Tamilalagan's study on fractional neutral stochastic integro-differential inclusions contributes to the literature by exploring approximate controllability through Mainardi's function, an important tool for addressing delays and stochasticity in fractional systems [10]. Podlubny's influential book on fractional differential equations presents a detailed treatment of the theory and applications of fractional calculus, making it an essential reference for understanding the foundational concepts used throughout this study [11]. Mainardi, Paradisi, and Gorenflo's work on probability distributions generated by fractional diffusion equations explores the connection between fractional derivatives and diffusion processes, providing valuable insights into the behavior of fractional systems [12]. In more recent studies, the existence and controllability of neutral fractional VFIDE are carried out by Gunasekar et al. while shedding light over the complexities presented by these kinds of systems to present new results for their solutions and control [13].

Hamoud's work on the existence and uniqueness of solutions for fractional neutral VFIDE provides key results in the theory of such systems, which ultimately guarantees well-posedness of these equations [15]. The further existence and uniqueness results for VFIDE by Hamoud, Mohammed, and Ghadle address the essential technical contributions in this field [16]. Gunasekar and colleagues recent analysis of existence, uniqueness and stability of neutral fractional VFIDE presents important results that contribute towards the theoretical foundations needed to be able to understand the stability of such complex systems [17]. Columbu, Frassu, and Viglialoro introduce refined criteria of boundedness related to chemotaxis systems relevant in the context of fractional nonlinear dynamics systems studies [18]. Hamoud and Ghadle's latest results regarding the uniqueness of solutions for fractional VFIDE bring in new perspectives regarding the structure and properties of such equations and the extension of understanding solutions to such equations [19]. The work done by Ndiaye and Mansal on the existence and uniqueness of results for VFIDE through the use of the Caputo fractional derivative has been critically useful in analyzing these types of equations [20].

Dahmani's work on high-dimensional fractional differential systems has introduced new results on existence and uniqueness that would help understand the more complex systems with fractional order [21]. HamaRashid et al. investigated the existence of Volterra-Fredholm integral equations of nonlinear boundary type with new numerical results that expand the understanding of boundary conditions in fractional systems [22]. This contributes to the impulsive fractional neutral stochastic integro-differential equation and understands such systems that produce both impulsive effects and stochastic behavior [23]. Lastly, the work by Hernandez, Prokopczyk, and Ladeira on partial functional differential equations with SDD gives additional theoretical basis in considering systems with delay and memory to further analyze important dynamics in those systems [24]. Through this body of work, this paper will contribute to the growing understanding of fractional VFIDE, especially with regard to controllability and SDDs. The research presented here extends the foundation of previous studies and introduces a new approach for solving these systems, opening new perspectives for future exploration.

Raghavendran et al. [25] deals with the existence, uniqueness, and stability of fractional neutral VFIDEs with state-dependent delays. The paper brings to the reader a few significant mathematical results on the types of systems discussed above as well as an insight into the behavior of these systems under particular conditions of state-dependent delays. These are critical to understand in systems governed by equivalent fractional equations when taken along with the control theory perspective. In this paper, we extend their findings by focusing on the controllability of systems described by such equations. More specifically, we investigate how state-dependent delays affect the ability to reach desired states when applying certain control strategies, utilizing the mathematical framework developed by Raghavendran et al. [25] to derive conditions for the controllability of the fractional systems under study.

In this study, we explore the controllability outcomes of mild solutions for a class of fractional neutral VFIDE with SDD, represented by the following system:

$$\begin{aligned} {}^{c}D^{\eta}\big(\varrho(\epsilon) - g_1(\epsilon, \varrho_{\rho(\epsilon,\varrho_\epsilon)})\big) &= \mathcal{A}\varrho(\epsilon) + g_2(\epsilon, \varrho_{\rho(\epsilon,\varrho_\epsilon)}) + \int_{\epsilon_0}^{\epsilon} Z_1(\epsilon, \xi, \varrho_{\rho(\xi,\varrho_s)})\, d\xi \\ &\quad + \int_{\epsilon_0}^{b} Z_2(\epsilon, \xi, \varrho_{\rho(\xi,\varrho_s)})\, d\xi + Bu(\epsilon), \quad \epsilon \in J = [\epsilon_0, b],\ 0 < \eta < 1, \end{aligned} \tag{1.1}$$

$$\varrho(\epsilon_0) = \varrho_0 = \varphi(\epsilon) \in \mathcal{B}, \quad \epsilon \in (-\infty, 0]. \tag{1.2}$$

The function $\varrho(\cdot)$ is an unknown function that maps values into a Banach space X, equipped with the norm $\|\cdot\|$. The Caputo fractional derivative ${}^{c}D^{\eta}$, of order $0 < \eta < 1$, is applied in the system. The operator $\mathcal{A}$ serves as the infinitesimal generator of a compact, analytic semigroup $\{T(\epsilon) : \epsilon \geq 0\}$, consisting of uniformly bounded linear operators acting on X. Let J represent the time interval, and define $D = \{(\epsilon, \xi) \in J \times J : \epsilon_0 \leq \xi \leq \epsilon \leq b\}$.

The functions $g_i : J \times \mathcal{B} \to X$ and $Z_i : D \times \mathcal{B} \to X$ (for $i = 1, 2$) are defined appropriately, while the function $\rho : J \times \mathcal{B} \to (-\infty, b]$ is also suitably specified. The initial condition $\varphi(0) = 0$ holds, where $\varphi \in \mathcal{B}$, and $\mathcal{B}$ is the phase space, as defined in the preliminary section.

The control function $u(\cdot)$ is an element of the Banach space $L^2(J, U)$, which includes admissible control functions, with U being another Banach space. The bounded linear operator $B : U \to X$ maps these control functions into the Banach space X. For any continuous function ϱ defined on $(-\infty, b]$ and any $\epsilon \geq 0$, the element ϱ_ϵ in $\mathcal{B}$ is defined by $\varrho_\epsilon(\theta) = \varrho(\epsilon + \theta)$ for $\theta \leq 0$, representing the state history from time $\theta \in (-\infty, 0]$ up to the current time ϵ.

2. Preliminaries

In this section, we focus on the commonly used definitions in fractional calculus, including the Riemann-Liouville fractional derivative and the Caputo derivative, as discussed in various academic studies [8, 14, 17, 24]. The Banach space $C(J, X)$, where $J = [\epsilon_0, \mathsf{b}]$, is endowed with the supremum norm. For any $\varrho \in C(J, X)$, this norm is expressed as $\|\varrho\|_\infty = \sup\{|\varrho(x)| : x \in J\}$.

Definition 2.1. [17, 24] Let $\eta > 0$ denote the order of integration, and let φ be a given function. The fractional integral of φ based on the Riemann-Liouville definition is expressed as

$$J^\eta \varphi(\tau) = \frac{1}{\Gamma(\eta)} \int_0^\tau (\tau - \epsilon)^{\eta - 1} \varphi(\epsilon)\, dt, \quad \text{for } \tau > 0 \text{ and } \eta \in \mathbb{R}^+,$$

where $\Gamma(\cdot)$ denotes the Gamma function, and $\mathbb{R}^+$ represents the set of positive real numbers. By convention, $J^0 \varphi(\tau) = \varphi(\tau)$.

Definition 2.2. [17, 24] The Caputo derivative of a function $\varphi : [0, 1) \to \mathbb{R}$, of order η within $0 < \eta < 1$, is defined as:

$$D^\eta \varphi(\tau) = \frac{1}{\Gamma(1 - \eta)} \int_0^\tau \frac{\varphi^{(0)}(\epsilon)}{(\tau - \epsilon)^\eta}\, dt, \quad \tau > 0.$$

Here, $\Gamma(1 - \eta)$ denotes the Gamma function evaluated at $1 - \eta$, and $\varphi^{(0)}(\epsilon)$ refers to the zeroth derivative (or the function φ itself).

Definition 2.3. [17, 24] For a function $\varphi(\tau)$, the Caputo fractional derivative is specified for an order η between $n - 1$ and n, where $n \in \mathbb{N}$. It is given by:

$${}^c D^\eta \varphi(\tau) = \frac{1}{\Gamma(n - \eta)} \int_0^\tau (\tau - \epsilon)^{n - \eta - 1} \frac{d^n \varphi(\epsilon)}{dt^n}\, dt, \quad n - 1 < \eta < n.$$

When $\eta = n$, the fractional derivative reduces to the standard n-th order derivative:

$${}^c D^\eta \varphi(\tau) = \frac{d^n \varphi(\tau)}{d\tau^n}.$$

The order η in this context can be real or even complex, representing the derivative's fractional order.

Theorem 2.1. (Schauder Fixed Point Theorem, see [13]) If a continuous mapping $N : B \to B$ has a relatively compact image in the Banach space E, then there exists at least one fixed point in the closed and convex subset B.

Theorem 2.2. (Arzelà-Ascoli Theorem, see [17]) On a closed and bounded interval $[a, b]$, any sequence of functions that is equicontinuous and bounded must possess a subsequence that converges uniformly.

This work incorporates an axiomatic definition for the phase space $\mathcal{B}$, similar to the frameworks described in [4]. The phase space $\mathcal{B}$ is defined as a linear space consisting of all mappings from $(-\infty, 0]$ to X. It is equipped with a seminorm $\|\cdot\|_{\mathcal{B}}$, satisfying the following axioms:

(A1) Let $\varrho : (-\infty, a] \to X$ be a function, where $a > 0$, continuous on J, and $\varrho_0 \in \mathcal{B}$. For every $\epsilon \in J$, the following properties hold:
  (i) The function ϱ_ϵ belongs to $\mathcal{B}$,
  (ii) $\|\varrho(\epsilon)\| \le H\|\varrho_\epsilon\|_{\mathcal{B}}$,
  (iii) $\|\varrho_\epsilon\|_{\mathcal{B}} \le K(\epsilon)\sup\{\|\varrho(\xi)\| : 0 \le \xi \le \epsilon\} + M(\epsilon)\|\varrho_0\|_{\mathcal{B}}$,
  where $H > 0$ is a constant, $K : [0, \infty) \to [1, \infty)$ is a continuous function, $M : [0, \infty) \to [1, \infty)$ is locally bounded, and the parameters H, K, and M are independent of $\varrho(\cdot)$.

(A2) For $\varrho(\cdot)$ defined in (A1), the function ϱ_ϵ is continuous and takes values in $\mathcal{B}$ on J.

(A3) The space $\mathcal{B}$ is complete.

3. Controllability Results for Fractional Neutral VFIDE with SDD

In this section, we analyze the controllability of mild solutions for fractional neutral VFIDE with SDD described by equations (1.1)-(1.2). Building upon the earlier discussion, we define the concept of a mild solution for these equations.

Definition 3.1. A function $\varrho : (-\infty, b] \to X$ is considered a mild solution of equations (1.1)-(1.2) if $\varrho_0 : \varphi \in \mathcal{B}$, and for each $\xi, \epsilon \in J$, it satisfies the following equation:

$$
\begin{aligned}
\varrho(\epsilon) = {}& S_\eta(\epsilon)(\varrho_0 - g_1(\epsilon_0, \varrho_0)) + g_1(\epsilon, \varrho_{\rho(\epsilon,\varrho_\epsilon)}) + \int_{\epsilon_0}^{\epsilon} T_\eta(\epsilon-\xi)(\epsilon-\xi)^{\eta-1} g_2(\xi, \varrho_{\rho(\epsilon,\varrho_s)})\,d\xi \\
&+ \int_{\epsilon_0}^{\epsilon} T_\eta(\epsilon-\xi)(\epsilon-\xi)^{\eta-1} \int_{\xi}^{\epsilon} Z_1(\tau, \xi, \varrho_{\rho(\epsilon,\varrho_s)})\,d\tau\,d\xi \\
&+ \int_{\epsilon_0}^{\epsilon} T_\eta(\epsilon-\xi)(\epsilon-\xi)^{\eta-1} \int_{\xi}^{b} Z_2(\tau, \xi, \varrho_{\rho(\epsilon,\varrho_s)})\,d\tau\,d\xi \\
&+ \int_{\epsilon_0}^{\epsilon} T_\eta(\epsilon-\xi)(\epsilon-\xi)^{\eta-1} B(\xi)u(\xi)d\xi,
\end{aligned}
\tag{3.1}
$$

where

$$S_\eta(\epsilon) = \int_0^\infty \phi_\eta(\theta) T(\epsilon^\eta \theta)\, d\theta, \qquad T_\eta(\epsilon) = \eta \int_0^\infty \theta \phi_\eta(\theta) T(\epsilon^\eta \theta)\, d\theta,$$

$$\phi_\eta(\theta) = \frac{1}{\eta}\theta^{-1-\frac{1}{\eta}}\psi_\eta(\theta^{-\frac{1}{\eta}}), \qquad \psi_\eta(\theta) = \frac{1}{\pi}\sum_{n=1}^{\infty}(-1)^{n-1}\theta^{-\eta n-1}\frac{\Gamma(n\eta+1)}{n!}\sin(n\pi\eta), \quad \theta \in (0,\infty),$$

and ϕ_η is a probability density function defined on $(0,\infty)$, satisfying

$$\phi_\eta(\theta) \geq 0, \quad \theta \in (0,\infty), \quad \text{and} \quad \int_0^\infty \phi_\eta(\theta)\, d\theta = 1.$$

Lemma 3.1. [25] The operators $S_\eta(\epsilon)$ and $T_\eta(\epsilon)$ exhibit the following properties for any $\epsilon \geq 0$:

(a) The operators S_η and T_η are linear and bounded for every fixed $\epsilon \geq 0$. Specifically, for any $\varrho \in X$, the following bounds apply:

$$\|S_\eta(\epsilon)\varrho\| \leq M\|\varrho\|, \quad \|T_\eta(\epsilon)\varrho\| \leq \frac{\eta M}{\Gamma(1+\eta)}\|\varrho\|.$$

(b) Both families $\{S_\eta(\epsilon) : \epsilon \geq 0\}$ and $\{T_\eta(\epsilon) : \epsilon \geq 0\}$ are strongly continuous.

(c) For any $\epsilon > 0$, the operators $S_\eta(\epsilon)$ and $T_\eta(\epsilon)$ are compact.

Definition 3.2. For any initial states ϱ_0 and ϱ_1 in the Banach space X, the system defined by equations (1.1)-(1.2) is considered controllable over the interval J if a control function $\delta(\epsilon)$ can be found within the space $L^2(J, U)$. The mild solution $\varrho(\epsilon)$ is ensured to satisfy the conditions $\varrho(\epsilon_0) = \varrho_0$ and $\varrho(b) = \varrho_1$ by this control function.

To derive our results, we assume the following conditions for the continuous function $\rho : J \times \mathcal{B} \to (-\infty, b]$:

(H1) For each $\epsilon > 0$, the semigroup $T(\epsilon)$ is compact.

(H2) The mappings $g_i : J \times \mathcal{B} \to X$ are continuous for $i = 1, 2$, and the following conditions hold:
For each $\epsilon \in J$ and any pair $(\vartheta, \vartheta_1) \in \mathcal{B}^2$, the following inequalities are satisfied:

$$\|g_1(\epsilon, \vartheta) - g_1(\epsilon, \vartheta_1)\|_X \leq L_{g_1}\|\vartheta - \vartheta_1\|_{\mathcal{B}},$$

$$\|g_2(\epsilon, \vartheta) - g_2(\epsilon, \vartheta_1)\|_X \leq L_{g_2}\|\vartheta - \vartheta_1\|_{\mathcal{B}}.$$

There exist constants $L^*_{g_1}$ and $L^*_{g_2}$ such that

$$L^*_{g_1} = \max_{\epsilon \in J}\|g_1(\epsilon, 0)\|_X, \quad L^*_{g_2} = \max_{\epsilon \in J}\|g_2(\epsilon, 0)\|_X.$$

(H3) The functions $Z_i : D \times \mathcal{B} \to X$ (for $i = 1, 2$) satisfy the following conditions: Continuity is ensured for $(\epsilon, \xi) \in D$ and $(\vartheta, \vartheta_1) \in \mathcal{B}^2$, with the following inequalities holding:

$$\|Z_1(\epsilon, \xi, \vartheta) - Z_1(\epsilon, \xi, \vartheta_1)\|_X \leq L_{Z_1}\|\vartheta - \vartheta_1\|_{\mathcal{B}},$$

$$\|Z_2(\epsilon, \xi, \vartheta) - Z_2(\epsilon, \xi, \vartheta_1)\|_X \leq L_{Z_2}\|\vartheta - \vartheta_1\|_{\mathcal{B}}.$$

There exist constants $L^*_{Z_1}$ and $L^*_{Z_2}$ such that:

$$L^*_{Z_1} = \max_{\epsilon, \xi \in D}\|Z_1(\epsilon, \xi, 0)\|_X, \quad L^*_{Z_2} = \max_{\epsilon, \xi \in D}\|Z_2(\epsilon, \xi, 0)\|_X.$$

(H4) The mapping $\epsilon \to \varphi_\epsilon$ is well-defined and continuous from $R(\rho^-) = \{\rho(\xi, \vartheta) : (\xi, \vartheta) \in J \times \mathcal{B}, \rho(\xi, \vartheta) \leq 0\}$ into $\mathcal{B}$. Additionally, there exists a bounded, continuous function $J^\varphi : R(\rho^-) \to (0, \infty)$ such that for every $\epsilon \in R(\rho^-)$,

$$\|\varphi_\epsilon\|_{\mathcal{B}} \leq J^\varphi(\epsilon)\|\varphi\|_{\mathcal{B}}.$$

(H5) The bounded linear operator $W : L^2(J, U) \to X$ is defined as

$$Wx = \frac{1}{\Gamma(\eta)} \int_{\epsilon_0}^{b} (b-\epsilon)^{\eta-1} Bu(\epsilon)\, dt,$$

where B satisfies $|B| \leq M_1$. Additionally, the operator W has an induced inverse W^{-1} acting within $\frac{L^2(J,U)}{\ker W}$, with a constant $M_2 > 0$ such that $|W^{-1}| \leq M_2$.

Theorem 3.1. Let the assumptions $(H1)$-$(H5)$ hold. Then, the system represented by equations (1.1) and (1.2) is controllable on the interval $[\epsilon_0, b]$.

Proof. Consider the collection of functions ϖ_l, defined as the set of all continuous functions ϱ mapping the interval J to the real numbers, such that $\|\varrho\|_\infty \leq l$. Utilizing the assumptions stated in hypothesis $(H5)$, a control can be derived by leveraging the properties of an arbitrary function $\varrho(\cdot)$, given as follows:

$$\begin{aligned}\mu(\epsilon) = W^{-1}\Bigg[&\varrho_1 - S_\eta(\epsilon)\big(\varrho_0 - g_1(\epsilon_0, \varrho_0)\big) - g_1(\epsilon, \varrho_{\rho(\epsilon,\varrho_\epsilon)})\\ &- \int_{\epsilon_0}^{\epsilon} T_\eta(\epsilon-\xi)(\epsilon-\xi)^{\eta-1}\Bigg[g_2(\xi, \varrho_{\rho(\epsilon,\varrho_s)}) + \int_{\xi}^{\epsilon} Z_1(\tau, \xi, \varrho_{\rho(\epsilon,\varrho_s)})\, d\tau\\ &+ \int_{\xi}^{b} Z_2(\tau, \xi, \varrho_{\rho(\epsilon,\varrho_s)})\, d\tau\Bigg] d\xi\Bigg](\epsilon).\end{aligned} \tag{3.2}$$

Using the defined control, we will demonstrate that the operator Φ, which maps the set ϖ_l to itself, is given by:

$$\begin{aligned}\Phi(\varrho)(\epsilon) = {}& S_\eta(\epsilon)\big(\varrho_0 - g_1(\epsilon_0, \varrho_0)\big) + g_1(\epsilon, \varrho_{\rho(\epsilon,\varrho_\epsilon)}) + \int_{\epsilon_0}^{\epsilon} T_\eta(\epsilon-\xi)(\epsilon-\xi)^{\eta-1} g_2(\xi, \varrho_{\rho(\epsilon,\varrho_s)})\, d\xi\\ &+ \int_{\epsilon_0}^{\epsilon} T_\eta(\epsilon-\xi)(\epsilon-\xi)^{\eta-1} \int_{\xi}^{\epsilon} Z_1(\tau, \xi, \varrho_{\rho(\epsilon,\varrho_s)})\, d\tau\, d\xi\\ &+ \int_{\epsilon_0}^{\epsilon} T_\eta(\epsilon-\xi)(\epsilon-\xi)^{\eta-1} \int_{\xi}^{b} Z_2(\tau, \xi, \varrho_{\rho(\epsilon,\varrho_s)})\, d\tau\, d\xi\\ &+ \int_{\epsilon_0}^{\epsilon} T_\eta(\epsilon-\xi)(\epsilon-\xi)^{\eta-1} B\mu(\xi)\, d\xi.\end{aligned} \tag{3.3}$$

We can deduce that a fixed point exists for the operator Φ, where $\mu(\epsilon)$ is defined as per equation (3.3). This fixed point corresponds to the mild solution of the control problem described by equations (1.1) and (1.2). Specifically, it is evident that $\Phi\, \varrho(b) = \varrho_1$, which indicates that the system represented by equations (1.1) and (1.2) is controllable over the interval $[\epsilon_0, b]$.

Since all the functions involved in the definition of the operator are continuous, we can conclude that the operator Φ is continuous. Expanding upon equation (3.1), for any function $\varrho \in \varpi_l$ and for all values of ϵ within the interval $[\epsilon_0, b]$, the following relationship holds:

$$\begin{aligned}
\mu(\epsilon) \leq \|W^{-1}\| \Bigg[& \|\varrho_1\| - \|S_\eta(\epsilon)\| \|\|\varrho_0\|\| - g_1(\epsilon_0, \varrho_0)\| + \|g_1(\epsilon, \varrho_{\rho(\epsilon,\varrho_\epsilon)})\| \\
& - \int_{\epsilon_0}^{\epsilon} T_\eta(\epsilon-\xi)\ (\epsilon-\xi)^{\eta-1} \Bigg[\|g_2(\xi, \varrho_{\rho(\epsilon,\varrho_s)})\| + \int_{\xi}^{\epsilon} \|Z_1(\tau, \xi, \varrho_{\rho(\epsilon,\varrho_s)})\| \, d\tau \\
& + \int_{\xi}^{b} \|Z_2(\tau, \xi, \varrho_{\rho(\epsilon,\varrho_s)})\| \, d\tau \Bigg] d\xi \Bigg] \\
\leq M_2 \Bigg[& \|\varrho_1\| + M\|\varrho_0\| + \|g_1(\epsilon, \varrho_{\rho(\epsilon,\varrho_\epsilon)})\| + \|g_1(\epsilon, \varrho_{\rho(\epsilon,\varrho_\epsilon)})\| \\
& + \frac{\eta M}{\Gamma(1+\eta)} \int_{\epsilon_0}^{\epsilon} (\epsilon-\xi)^{\eta-1} \|g_2(\xi, \varrho_{\rho(\epsilon,\varrho_s)})\| \, d\xi \\
& + \frac{\eta M}{\Gamma(1+\eta)} \int_{\epsilon_0}^{\epsilon} (\epsilon-\xi)^{\eta-1} \int_{\xi}^{\epsilon} \|Z_1(\tau, \xi, \varrho_{\rho(\epsilon,\varrho_s)})\| \, d\tau \, d\xi \\
& + \frac{\eta M}{\Gamma(1+\eta)} \int_{\epsilon_0}^{\epsilon} (\epsilon-\xi)^{\eta-1} \int_{\xi}^{b} \|Z_2(\tau, \xi, \varrho_{\rho(\epsilon,\varrho_s)})\| \, d\tau \, d\xi \Bigg] \\
\leq M_2 \Bigg[& \|\varrho_1\| + M\|\varrho_0\| + \|g_1(\epsilon, \varrho_{\rho(\epsilon,\varrho_\epsilon)})\| + L_{g_1}\|\varrho_{\rho(\xi,\bar{\varrho}_s)}\|_{\mathcal{B}} + L^*_{g_1} \\
& + \frac{\eta M}{\Gamma(1+\eta)} \int_{\epsilon_0}^{\epsilon} (\epsilon-\xi)^{\eta-1} \Bigg[L_{g_2}\|\varrho_{\rho(\xi,\bar{\varrho}_s)}\|_{\mathcal{B}} + L^*_{g_2} + \int_{\xi}^{\epsilon} (L_{Z_1}\|\varrho_{\rho(\xi,\bar{\varrho}_s)}\|_{\mathcal{B}} + L^*_{Z_1}) d\tau \\
& + \int_{\xi}^{b} (L_{Z_2}\|\varrho_{\rho(\xi,\bar{\varrho}_s)}\|_{\mathcal{B}} + L^*_{Z_2}) d\tau \Bigg] d\xi \Bigg] \\
\leq M_2 \Bigg[& \|\varrho_1\| + M\|\varrho_0\| + \|g_1(\epsilon, \varrho_{\rho(\epsilon,\varrho_\epsilon)})\| + L_{g_1} r^* + L^*_{g_1} + \frac{Me^\eta}{\Gamma(1+\eta)}\ (L_{g_2} r^* + L^*_{g_2}) \\
& + \frac{Me^{\eta+1}}{(\eta+1)\Gamma(\eta)} (L_{Z_1} r^* + L^*_{Z_1}) + \frac{Me^{\eta+1}}{(\eta+1)\Gamma(\eta)} (L_{Z_2} r^* + L^*_{Z_2}) \Bigg] \\
\leq M_2 \Bigg[& \|\varrho_1\| + M\|\varrho_0\| + \|g_1(\epsilon, \varrho_{\rho(\epsilon,\varrho_\epsilon)})\| + L_{g_1} r^* + L^*_{g_1} + Me^\eta \Bigg[\frac{L_{g_2}}{\Gamma(\eta+1)} + \frac{e(L_{Z_1} + L_{Z_2})}{(\eta+1)\Gamma(\eta)} \Bigg] r^* \\
& + Me^\eta \Bigg[\frac{L^*_{g_2}}{\Gamma(\eta+1)} + \frac{e(L^*_{Z_1} + L^*_{Z_2})}{(\eta+1)\Gamma(\eta)} \Bigg] \Bigg].
\end{aligned}$$

Applying the equations (3.2) and (3.3), we can derive the following result:

$$\|\Phi(\varrho)(\epsilon)\| \leq M\|\varrho_0\| + \|g_1(\epsilon, \varrho_{\rho(\epsilon,\varrho_\epsilon)})\| + \|g_1(\epsilon, \varrho_{\rho(\epsilon,\varrho_\epsilon)})\| + \frac{\eta M}{\Gamma(1+\eta)} \int_{\epsilon_0}^{\epsilon} (\epsilon-\xi)^{\eta-1} \|g_2(\xi, \varrho_{\rho(\epsilon,\varrho_s)})\| \, d\xi$$

$$
\begin{aligned}
&+\frac{\eta M}{\Gamma(1+\eta)}\int_{\epsilon_0}^{\epsilon}(\epsilon-\xi)^{\eta-1}\\
&\int_{\xi}^{\epsilon}\|Z_1(\tau,\xi,\varrho_{\rho(\epsilon,\varrho_s)})\|\,d\tau\,d\xi+\frac{\eta M}{\Gamma(1+\eta)}\int_{\epsilon_0}^{\epsilon}(\epsilon-\xi)^{\eta-1}\int_{\xi}^{b}\|Z_2(\tau,\xi,\varrho_{\rho(\epsilon,\varrho_s)})\|\,d\tau\,d\xi\\
&+\frac{\eta M}{\Gamma(1+\eta)}\int_{\epsilon_0}^{\epsilon}(\epsilon-\xi)^{\eta-1}\|B\|\|\mu(\epsilon)\|\\
\le{}& M\|\varrho_0\|+\|g_1(\epsilon,\varrho_{\rho(\epsilon,\varrho_\epsilon)})\|+L_{g_1}\|\varrho_{\rho(\xi,\bar{\varrho}_s)}\|_{\mathcal{B}}+L^*_{g_1}\\
&+\frac{\eta M}{\Gamma(1+\eta)}\int_{\epsilon_0}^{\epsilon}(\epsilon-\xi)^{\eta-1}\Bigg[L_{g_2}\|\varrho_{\rho(\xi,\bar{\varrho}_s)}\|_{\mathcal{B}}+L^*_{g_2}+\int_{\xi}^{\epsilon}(L_{Z_1}\|\varrho_{\rho(\xi,\bar{\varrho}_s)}\|_{\mathcal{B}}+L^*_{Z_1})d\tau\\
&+\int_{\xi}^{b}(L_{Z_2}\|\varrho_{\rho(\xi,\bar{\varrho}_s)}\|_{\mathcal{B}}+L^*_{Z_2})d\tau\Bigg]d\xi+\frac{\eta M}{\Gamma(1+\eta)}\int_{\epsilon_0}^{\epsilon}(\epsilon-\xi)^{\eta-1}M_1\|\mu(\epsilon)\|\\
\le{}& M\|\varrho_0\|+\|g_1(\epsilon,\varrho_{\rho(\epsilon,\varrho_\epsilon)})\|+L_{g_1}r^*+L^*_{g_1}\\
&+\frac{Me^{\eta}}{\Gamma(1+\eta)}(L_{g_2}r^*+L^*_{g_2})+\frac{Me^{\eta+1}}{(\eta+1)\Gamma(\eta)}(L_{Z_1}r^*+L^*_{Z_1})\\
&+\frac{Me^{\eta+1}}{(\eta+1)\Gamma(\eta)}(L_{Z_2}r^*+L^*_{Z_2})+\frac{Me^{\eta}}{\Gamma(1+\eta)}M_1M_2\Bigg[\|\varrho_1\|-M\|\varrho_0\|+\|g_1(\epsilon,\varrho_{\rho(\epsilon,\varrho_\epsilon)})\|\\
&+L_{g_1}r^*+L^*_{g_1}+\frac{Me^{\eta}}{\Gamma(1+\eta)}(L_{g_2}r^*+L^*_{g_2})+\frac{Me^{\eta+1}}{(\eta+1)\Gamma(\eta)}(L_{Z_1}r^*\\
&+L^*_{Z_1})+\frac{Me^{\eta+1}}{(\eta+1)\Gamma(\eta)}(L_{Z_2}r^*+L^*_{Z_2})\Bigg]\\
\le{}& M\|\varrho_0\|+\|g_1(\epsilon,\varrho_{\rho(\epsilon,\varrho_\epsilon)})\|+L_{g_1}r^*+L^*_{g_1}\\
&+Me^{\eta}\left[\frac{L_{g_2}}{\Gamma(\eta+1)}+\frac{e(L_{Z_1}+L_{Z_2})}{(\eta+1)\Gamma(\eta)}\right]r^*+Me^{\eta}\left[\frac{L^*_{g_2}}{\Gamma(\eta+1)}+\frac{e(L^*_{Z_1}+L^*_{Z_2})}{(\eta+1)\Gamma(\eta)}\right]\\
&+\frac{Me^{\eta}}{\Gamma(1+\eta)}M_1M_2\Bigg[\|\varrho_1\|+M\|\varrho_0\|+\|g_1(\epsilon,\varrho_{\rho(\epsilon,\varrho_\epsilon)})\|+L_{g_1}r^*+L^*_{g_1}\\
&+Me^{\eta}\left[\frac{L_{g_2}}{\Gamma(\eta+1)}+\frac{e(L_{Z_1}+L_{Z_2})}{(\eta+1)\Gamma(\eta)}\right]r^*+Me^{\eta}\left[\frac{L^*_{g_2}}{\Gamma(\eta+1)}+\frac{e(L^*_{Z_1}+L^*_{Z_2})}{(\eta+1)\Gamma(\eta)}\right]\Bigg]\\
\le{}& \frac{Me^{\eta}}{\Gamma(1+\eta)}M_1M_2\|\varrho_1\|+\left(1+\frac{Me^{\eta}}{\Gamma(1+\eta)}M_1M_2\right)\Bigg[M\|\varrho_0\|+\|g_1(\epsilon,\varrho_{\rho(\epsilon,\varrho_\epsilon)})\|\\
&+L_{g_1}r^*+L^*_{g_1}+Me^{\eta}\left[\frac{L_{g_2}}{\Gamma(\eta+1)}+\frac{e(L_{Z_1}+L_{Z_2})}{(\eta+1)\Gamma(\eta)}\right]r^*+Me^{\eta}\left[\frac{L^*_{g_2}}{\Gamma(\eta+1)}+\frac{e(L^*_{Z_1}+L^*_{Z_2})}{(\eta+1)\Gamma(\eta)}\right]\Bigg].
\end{aligned}
$$

Thus,

$$
\|\Phi(\varrho)\|_\infty \le \frac{Me^{\eta}}{\Gamma(1+\eta)}M_1M_2\|\varrho_1\|+\left(1+\frac{Me^{\eta}}{\Gamma(1+\eta)}M_1M_2\right)\Bigg[M\|\varrho_0\|+\|g_1(\epsilon,\varrho_{\rho(\epsilon,\varrho_\epsilon)})\|+L_{g_1}r^*+L^*_{g_1}
$$

$$+Me^{\eta}\left[\frac{L_{g_2}}{\Gamma(\eta+1)}+\frac{e(L_{Z_1}+L_{Z_2})}{(\eta+1)\Gamma(\eta)}\right]r^{*}+Me^{\eta}\left[\frac{L^{*}_{g_2}}{\Gamma(\eta+1)}+\frac{e(L^{*}_{Z_1}+L^{*}_{Z_2})}{(\eta+1)\Gamma(\eta)}\right]\Bigg]:=l.$$

We conclude that $\|\Phi\varrho\|\le l$, which implies that $\Phi\varrho\in\varpi_l$. Therefore, it follows that $\Phi\varpi_l\subset\varpi_l$. This establishes that the operator Φ maps the set $\varpi_l=\{\varrho\in C(J,X):\|\varrho\|_\infty\le l\}$ onto itself. Next, we will demonstrate that the operator $\Phi:\varpi_l\to\varpi_l$ satisfies all the conditions of (2.1). The proof will be carried out in several steps.

Step 1: The operator Φ is continuous. Let $\{\varrho_n\}$ be a sequence such that $\varrho_n\to\varrho$ in ϖ_l,

$$\begin{aligned}\|\Phi\varrho_n(\epsilon)-\Phi\varrho(\epsilon)\|\le{}&\|g_1(\xi,\varrho_{n\rho(\epsilon,\varrho_s)})-g_1(\xi,\varrho_{\rho(\epsilon,\varrho_s)})\|\\
&+\int_{\epsilon_0}^{\epsilon}T_\eta(\epsilon-\xi)(\epsilon-\xi)^{\eta-1}\|g_2(\xi,\varrho_{n\rho(\epsilon,\varrho_s)})-g_2(\xi,\varrho_{\rho(\epsilon,\varrho_s)})\|\,d\xi\\
&+\int_{\epsilon_0}^{\epsilon}T_\eta(\epsilon-\xi)(\epsilon-\xi)^{\eta-1}\int_{\xi}^{\epsilon}\|Z_1(\tau,\xi,\varrho_{n\rho(\epsilon,\varrho_s)})-Z_1(\tau,\xi,\varrho_{\rho(\epsilon,\varrho_s)})\|\,d\tau\,d\xi\\
&+\int_{\epsilon_0}^{\epsilon}T_\eta(\epsilon-\xi)(\epsilon-\xi)^{\eta-1}\int_{\xi}^{b}\|Z_2(\tau,\xi,\varrho_{n\rho(\epsilon,\varrho_s)})-Z_2(\tau,\xi,\varrho_{\rho(\epsilon,\varrho_s)})\|\,d\tau\,d\xi\\
&+\int_{\epsilon_0}^{\epsilon}T_\eta(\epsilon-\xi)(\epsilon-\xi)^{\eta-1}BW^{-1}\Bigg[\|g_1(\xi,\varrho_{n\rho(\epsilon,\varrho_s)})-g_1(\xi,\varrho_{\rho(\epsilon,\varrho_s)})\|\\
&+\int_{\epsilon_0}^{\epsilon}T_\eta(\epsilon-\xi)(\epsilon-\xi)^{\eta-1}\|g_2(\xi,\varrho_{n\rho(\epsilon,\varrho_s)})\\
&-g_2(\xi,\varrho_{\rho(\epsilon,\varrho_s)})\|\,d\xi+\int_{\epsilon_0}^{\epsilon}T_\eta(\epsilon-\xi)(\epsilon-\xi)^{\eta-1}\int_{\xi}^{\epsilon}\|Z_1(\tau,\xi,\varrho_{n\rho(\epsilon,\varrho_s)})\\
&-Z_1(\tau,\xi,\varrho_{\rho(\epsilon,\varrho_s)})\|\,d\tau\,d\xi+\int_{\epsilon_0}^{\epsilon}T_\eta(\epsilon-\xi)(\epsilon-\xi)^{\eta-1}\int_{\xi}^{b}\|Z_2(\tau,\xi,\varrho_{n\rho(\epsilon,\varrho_s)})\\
&-Z_2(\tau,\xi,\varrho_{\rho(\epsilon,\varrho_s)})\|\,d\tau\,d\xi\Bigg]d\xi\end{aligned}$$

Due to the continuity of g, Z_1, and Z_2, it follows that $\|\Phi\varrho_n(\epsilon)-\Phi\varrho(\epsilon)\|\to 0$ as $n\to\infty$. Hence, the operator Φ is continuous on the set ϖ_l.

Step 2: The set $\Phi(\varpi_l)$ is uniformly bounded. This is clear because $\Phi(\varpi_l)\subset\varpi_l$, implying that $\Phi(\varpi_l)$ is bounded.

Step 3: We now demonstrate that $\Phi(\varpi_l)$ is equicontinuous.

Consider ϵ_1 and ϵ_2 in the bounded set $[\epsilon_0,b]\subset C(J,X)$, as described in Step 2, along with $\varrho\in\varpi_l$ and $\epsilon_1<\epsilon_2$. In this context, we have:

$$\begin{aligned}&\|(\Phi\varrho)(\epsilon_2)-(\Phi\varrho)(\epsilon_1)\|\\
={}&\Bigg\|S_\eta(\epsilon_2)\,(\varrho_0-g_1(\epsilon_0,\varrho_0))+g_1(\epsilon,\varrho_{\rho(\epsilon,\varrho_\epsilon)})\\
&+\int_{\epsilon_0}^{\epsilon_2}T_\eta(\epsilon_2-\xi)(\epsilon_2-\xi)^{\eta-1}g_2(\xi,\varrho_{\rho(\xi,\varrho_s)})\,d\xi\end{aligned}$$

$$
\begin{aligned}
& + \int_{\epsilon_0}^{\epsilon_2} (\epsilon_2 - \xi)^{\eta-1} T_\eta(\epsilon_2 - \xi) \int_{\xi}^{\epsilon_2} Z_1(\tau, \xi, \varrho_{\rho(\xi,\varrho_s)}) d\tau d\xi \\
& + \int_{\epsilon_0}^{\epsilon_2} (\epsilon_2 - \xi)^{\eta-1} T_\eta(\epsilon_2 - \xi) \int_{\xi}^{b} Z_2(\tau, \xi, \varrho_{\rho(\xi,\varrho_s)}) d\tau d\xi \\
& + \int_{\epsilon_0}^{\epsilon_2} (\epsilon_2 - \xi)^{\eta-1} T_\eta(\epsilon_2 - \xi) B W^{-1} \Big[\varrho_1 - S_\eta(\epsilon_2)\, (\varrho_0 - g_1(\epsilon_0, \varrho_0)) + g_1(\epsilon, \varrho_{\rho(\epsilon,\varrho_\epsilon)}) \\
& - \int_{\epsilon_0}^{\epsilon_2} T_\eta(\epsilon_2 - \xi)\, (\epsilon_2 - \xi)^{\eta-1} \Big[g_2(\xi, \varrho_{\rho(\xi,\varrho_s)}) \\
& + \int_{\xi}^{\epsilon_2} Z_1(\tau, \xi, \varrho_{\rho(\epsilon_2,\varrho_s)})\, d\tau + \int_{\xi}^{b} Z_2(\tau, \xi, \varrho_{\rho(\epsilon_2,\varrho_s)})\, d\tau \Big] d\xi \Big] \\
& - S_\eta(\epsilon_1)\, (\varrho_0 - g_1(\epsilon_0, \varrho_0)) + g_1(\epsilon, \varrho_{\rho(\epsilon,\varrho_\epsilon)}) \\
& - \int_{\epsilon_0}^{\epsilon_1} T_\eta(\epsilon_1 - \xi)(\epsilon_1 - \xi)^{\eta-1} g_2(\xi, \varrho_{\rho(\xi,\varrho_s)})\, d\xi \\
& - \int_{\epsilon_0}^{\epsilon_1} (\epsilon_1 - \xi)^{\eta-1} T_\eta(\epsilon_1 - \xi) \int_{\xi}^{\epsilon_1} Z_1(\tau, \xi, \varrho_{\rho(\xi,\varrho_s)}) d\tau d\xi \\
& - \int_{\epsilon_0}^{\epsilon_1} (\epsilon_1 - \xi)^{\eta-1} T_\eta(\epsilon_1 - \xi) \int_{\xi}^{b} Z_2(\tau, \xi, \varrho_{\rho(\xi,\varrho_s)}) d\tau d\xi \\
& - \int_{\epsilon_0}^{\epsilon_1} (\epsilon_1 - \xi)^{\eta-1} T_\eta(\epsilon_1 - \xi) B W^{-1} \Big[\varrho_1 - S_\eta(\epsilon_1)\, (\varrho_0 - g_1(\epsilon_0, \varrho_0)) + g_1(\epsilon, \varrho_{\rho(\epsilon,\varrho_\epsilon)}) \\
& - \int_{\epsilon_0}^{\epsilon_1} T_\eta(\epsilon_1 - \xi)\, (\epsilon_1 - \xi)^{\eta-1} \Big[g_2(\xi, \varrho_{\rho(\xi,\varrho_s)}) \\
& + \int_{\xi}^{\epsilon_1} Z_1(\tau, \xi, \varrho_{\rho(\epsilon_1,\varrho_s)})\, d\tau + \int_{\xi}^{b} Z_2(\tau, \xi, \varrho_{\rho(\epsilon_1,\varrho_s)})\, d\tau \Big] d\xi \Big] \Big\| \\
\leq \;& \frac{M\eta}{\Gamma(1+\eta)} \Big\| g_1(\epsilon, \varrho_{\rho(\epsilon,\varrho_\epsilon)}) + \int_{\epsilon_1}^{\epsilon_2} (\epsilon_2 - \xi)^{\eta-1} g_2(\xi, \varrho_{\rho(\xi,\varrho_s)}) d\xi \\
& + \int_{\epsilon_1}^{\epsilon_2} (\epsilon_2 - \xi)^{\eta-1} \int_{\xi}^{\epsilon_2} Z_1(\tau, \xi, \varrho_{\rho(\xi,\varrho_s)}) d\tau d\xi \\
& + \int_{\epsilon_1}^{\epsilon_2} (\epsilon_2 - \xi)^{\eta-1} \int_{\xi}^{b} Z_2(\tau, \xi, \varrho_{\rho(\xi,\varrho_s)}) d\tau d\xi \\
& - \int_{\epsilon_0}^{\epsilon_1} (\epsilon_1 - \xi)^{\eta-1} g_2(\xi, \varrho_{\rho(\xi,\varrho_s)}) d\xi \\
& - \int_{\epsilon_0}^{\epsilon_1} (\epsilon_1 - \xi)^{\eta-1} \int_{\xi}^{\epsilon_1} Z_1(\tau, \xi, \varrho_{\rho(\xi,\varrho_s)}) d\tau d\xi \\
& - \int_{\epsilon_0}^{\epsilon_1} (\epsilon_1 - \xi)^{\eta-1} \int_{\xi}^{b} Z_2(\tau, \xi, \varrho_{\rho(\xi,\varrho_s)}) d\tau d\xi \\
& + \int_{\epsilon_0}^{\epsilon_1} (\epsilon_2 - \xi)^{\eta-1} g_2(\xi, \varrho_{\rho(\xi,\varrho_s)}) d\xi
\end{aligned}
$$

$$
\begin{aligned}
& + \int_{\epsilon_0}^{\epsilon_1} (\epsilon_2 - \xi)^{\eta-1} \int_{\xi}^{\epsilon_2} Z_1(\tau, \xi, \varrho_{\rho(\xi,\varrho_s)}) d\tau d\xi \\
& + \int_{\epsilon_0}^{\epsilon_1} (\epsilon_2 - \xi)^{\eta-1} \int_{\xi}^{b} Z_2(\tau, \xi, \varrho_{\rho(\xi,\varrho_s)}) d\tau d\xi \\
& + BW^{-1}\Bigg[g_1(\epsilon, \varrho_{\rho(\epsilon,\varrho_\epsilon)}) + \int_{\epsilon_1}^{\epsilon_2} (\epsilon_2 - \xi)^{\eta-1} g_2(\xi, \varrho_{\rho(\xi,\varrho_s)}) d\xi \\
& + \int_{\epsilon_1}^{\epsilon_2} (\epsilon_2 - \xi)^{\eta-1} \int_{\xi}^{\epsilon_2} Z_1(\tau, \xi, \varrho_{\rho(\xi,\varrho_s)}) d\tau d\xi \\
& + \int_{\epsilon_1}^{\epsilon_2} (\epsilon_2 - \xi)^{\eta-1} \int_{\xi}^{b} Z_2(\tau, \xi, \varrho_{\rho(\xi,\varrho_s)}) d\tau d\xi \\
& - \int_{\epsilon_0}^{\epsilon_1} (\epsilon_1 - \xi)^{\eta-1} g_2(\xi, \varrho_{\rho(\xi,\varrho_s)}) d\xi \\
& - \int_{\epsilon_0}^{\epsilon_1} (\epsilon_1 - \xi)^{\eta-1} \int_{\xi}^{\epsilon_1} Z_1(\tau, \xi, \varrho_{\rho(\xi,\varrho_s)}) d\tau d\xi \\
& - \int_{\epsilon_0}^{\epsilon_1} (\epsilon_1 - \xi)^{\eta-1} \int_{\xi}^{b} Z_2(\tau, \xi, \varrho_{\rho(\xi,\varrho_s)}) d\tau d\xi \\
& + \int_{\epsilon_0}^{\epsilon_1} (\epsilon_2 - \xi)^{\eta-1} g_2(\xi, \varrho_{\rho(\xi,\varrho_s)}) d\xi \\
& + \int_{\epsilon_0}^{\epsilon_1} (\epsilon_2 - \xi)^{\eta-1} \int_{\xi}^{\epsilon_2} Z_1(\tau, \xi, \varrho_{\rho(\xi,\varrho_s)}) d\tau d\xi \\
& + \int_{\epsilon_0}^{\epsilon_1} (\epsilon_2 - \xi)^{\eta-1} \int_{\xi}^{b} Z_2(\tau, \xi, \varrho_{\rho(\xi,\varrho_s)}) d\tau d\xi \Bigg]\Bigg\| \\
\leq\ & \frac{M\eta}{\Gamma(1+\eta)} \Bigg\| g_1(\epsilon, \varrho_{\rho(\epsilon,\varrho_\epsilon)}) + \int_{\epsilon_1}^{\epsilon_2} (\epsilon_2 - \xi)^{\eta-1} \Bigg[g_2(\xi, \varrho_{\rho(\xi,\varrho_s)}) + \int_{\xi}^{\epsilon_2} Z_1(\tau, \xi, \varrho_{\rho(\xi,\varrho_s)}) d\tau \\
& + \int_{\xi}^{b} Z_2(\tau, \xi, \varrho_{\rho(\xi,\varrho_s)}) d\tau \Bigg] d\xi \\
& - \int_{\epsilon_0}^{\epsilon_1} (\epsilon_1 - \xi)^{\eta-1} g_2(\xi, \varrho_{\rho(\xi,\varrho_s)}) d\xi + \int_{\epsilon_0}^{\epsilon_1} (\epsilon_2 - \xi)^{\eta-1} g_2(\xi, \varrho_{\rho(\xi,\varrho_s)}) d\xi \\
& - \int_{\epsilon_0}^{\epsilon_1} \Bigg[(\epsilon_1 - \xi)^{\eta-1} \int_{\xi}^{\epsilon_1} Z_1(\tau, \xi, \varrho_{\rho(\xi,\varrho_s)}) d\tau \\
& - (\epsilon_2 - \xi)^{\eta-1} \int_{\xi}^{\epsilon_2} Z_1(\tau, \xi, \varrho_{\rho(\xi,\varrho_s)}) d\tau \Bigg] d\xi - \int_{\epsilon_0}^{\epsilon_1} \Bigg[(\epsilon_1 - \xi)^{\eta-1} \\
& \int_{\xi}^{b} Z_2(\tau, \xi, \varrho_{\rho(\xi,\varrho_s)}) d\tau - (\epsilon_2 - \xi)^{\eta-1} \int_{\xi}^{b} Z_2(\tau, \xi, \varrho_{\rho(\xi,\varrho_s)}) d\tau \Bigg] d\xi \\
& + BW^{-1}\Bigg[g_1(\epsilon, \varrho_{\rho(\epsilon,\varrho_\epsilon)}) + \int_{\epsilon_1}^{\epsilon_2} (\epsilon_2 - \xi)^{\eta-1} \Bigg[g_2(\xi, \varrho_{\rho(\xi,\varrho_s)}) + \int_{\xi}^{\epsilon_2} Z_1(\tau, \xi, \varrho_{\rho(\xi,\varrho_s)}) d\tau
\end{aligned}
$$

$$+ \int_{\xi}^{b} Z_2(\tau, \xi, \varrho_{\rho(\xi,\varrho_s)}) d\tau \Big] d\xi$$
$$- \int_{\epsilon_0}^{\epsilon_1} (\epsilon_1 - \xi)^{\eta-1} g_2(\xi, \varrho_{\rho(\xi,\varrho_s)}) d\xi + \int_{\epsilon_0}^{\epsilon_1} (\epsilon_2 - \xi)^{\eta-1} g_2(\xi, \varrho_{\rho(\xi,\varrho_s)}) d\xi$$
$$- \int_{\epsilon_0}^{\epsilon_1} \Big[(\epsilon_1 - \xi)^{\eta-1} \int_{\xi}^{\epsilon_1} Z_1(\tau, \xi, \varrho_{\rho(\xi,\varrho_s)}) d\tau$$
$$-(\epsilon_2 - \xi)^{\eta-1} \int_{\xi}^{\epsilon_2} Z_1(\tau, \xi, \varrho_{\rho(\xi,\varrho_s)}) d\tau \Big] d\xi - \int_{\epsilon_0}^{\epsilon_1} \Big[(\epsilon_1 - \xi)^{\eta-1}$$
$$\int_{\xi}^{b} Z_2(\tau, \xi, \varrho_{\rho(\xi,\varrho_s)}) d\tau - (\epsilon_2 - \xi)^{\eta-1} \int_{\xi}^{b} Z_2(\tau, \xi, \varrho_{\rho(\xi,\varrho_s)}) d\tau \Big] d\xi \Big] \Big\|$$

As $\epsilon_2 - \epsilon_1 \to 0$, the right-hand side tends to zero. Since $T_\eta(\epsilon)$ forms a strongly continuous semigroup for $\epsilon \geq 0$ and is compact for $\epsilon > 0$, it follows that $T_\eta(\epsilon)$ is continuous in the uniform operator topology for $\epsilon > 0$. Consequently, the equicontinuity for the other cases, such as $\epsilon_1 < \epsilon_2 \leq 0$ or $\epsilon_1 \leq 0 \leq \epsilon_2 \leq b$, can be deduced without difficulty.

By combining the results of Steps 1-3 and applying Theorem (2.2), we establish that the operator Φ is both continuous and compact. Therefore, utilizing Theorem (2.1), we conclude that a fixed point ϱ exists, which serves as a solution to the problem defined by equations (1.1) and (1.2). Hence, the system described by these equations is controllable on the interval $J = [\epsilon_0, b]$. This completes the proof of the theorem. □

4. Example

As an illustrative example, we examine a control system described by the fractional neutral VFIDE with SDD as follows:

$$\begin{aligned} {}^{c}D^{\eta}\Big[x(\epsilon) - \int_{-\infty}^{\epsilon} \frac{e^{2(\xi-\epsilon)} x(\xi - \rho_1(\xi)\rho_2(\|x(\xi)\|))}{25} d\xi\Big] &= \frac{\partial^2}{\partial \varrho^2}\Big[x(\epsilon) + \mu(\epsilon) \\ &+ \int_{-\infty}^{\epsilon} \frac{e^{2(\xi-\epsilon)} x(\xi - \rho_1(\xi)\rho_2(\|x(\xi)\|))}{64} d\xi \\ &+ \int_{-\infty}^{\epsilon} \frac{e^{2(\tau-\xi)} x(\tau - \rho_1(\tau)\rho_2(\|x(\tau)\|))}{16} d\tau\, d\xi \\ &+ \int_{0}^{\epsilon} \sin(\epsilon - \xi) \int_{-\infty}^{\xi} \frac{e^{2(\tau-\xi)} x(\tau - \rho_1(\tau)\rho_2(\|x(\tau)\|))}{36} d\tau\, d\xi \\ &+ \int_{0}^{\epsilon} \sin(\epsilon - \xi) \int_{-\infty}^{\xi} \frac{e^{2(\tau-\xi)} x(\tau - \rho_1(\tau)\rho_2(\|x(\tau)\|))}{36} d\tau\, d\xi, \Big] \end{aligned} \tag{4.1}$$

with boundary conditions

$$x(\epsilon, 0) = 0 = x(\epsilon, \pi), \quad \epsilon \in [0, b], \tag{4.2}$$

and initial condition

$$x(\epsilon) = \varphi(\epsilon), \quad \epsilon \leq 0, \quad \varrho \in [0, \pi]. \tag{4.3}$$

Consider the operator $\mathcal{A} : D(\mathcal{A}) \subset X \to X$, where $X = L^2[0,\pi]$ with the L^2-norm $\|\cdot\|_{L^2}$, and let ${}^cD_\epsilon^\eta$ represent the Caputo fractional derivative of order $\eta \in (0,1)$. Suppose $\varphi \in \mathcal{B}$. The action of the operator $\mathcal{A}$ is defined as $\mathcal{A}\sigma = \sigma''$, where the domain $D(\mathcal{A})$ consists of functions $\sigma \in X$ such that σ and σ' are absolutely continuous, $\sigma'' \in X$, and the boundary conditions $\sigma(0) = \sigma(\pi) = 0$ are satisfied.

We can express $\mathcal{A}\sigma$ as:

$$\mathcal{A}\sigma = \sum_{n=1}^{\infty} n^2 \langle \sigma, \sigma_n \rangle \sigma_n, \quad \text{for } \sigma \in D(\mathcal{A}),$$

where the functions $\sigma_n(\xi) = \sqrt{\frac{2}{\pi}} \sin(ns)$ for $n = 1, 2, \ldots$ form an orthogonal set of eigenvectors for the operator $\mathcal{A}$. It is well-established that $\mathcal{A}$ generates an analytic semigroup $\{T(\epsilon)\}_{\epsilon \geq 0}$ in the space X, which is expressed as:

$$T(\epsilon)\sigma = \sum_{n=1}^{\infty} e^{-n^2\epsilon} \langle \sigma, \sigma_n \rangle \sigma_n, \quad \text{for every } \sigma \in X \text{ and } \epsilon > 0.$$

Since the semigroup $\{T(\epsilon)\}_{\epsilon \geq 0}$ is analytic and compact, there exists a constant $M > 0$ such that $\|T(\epsilon)\|_{L(X)} \leq M$. For the phase space, we select $x = e^{2s}$ for $\xi < 0$, which yields $l = \int_{-\infty}^{0} x(\xi)\, d\xi = \frac{1}{2} < \infty$ for $\epsilon \leq 0$. Additionally, we define the norm:

$$\|\sigma\|_{\mathcal{B}} = \int_{-\infty}^{0} x(\xi) \sup_{\theta \in [\xi, 0]} \|\sigma(\theta)\|_{L^2}\, d\xi.$$

Thus, for $(\epsilon, \varphi) \in [0,b] \times \mathcal{B}$, where $\varphi(\theta)(\varrho) = \varphi(\theta)$ for $(\theta) \in (-\infty, 0] \times [0,\pi]$, we define $x(\epsilon)(\varrho) = x(\epsilon)$ and $\rho(\epsilon,\varphi) = \rho_1(\epsilon)\rho_2(\|\varphi(0)\|)$. Consequently, we have:

$$g_1(\epsilon,\varphi)(\varrho) = \int_{-\infty}^{0} e^{2(\xi)} \frac{\varphi}{25} d\xi$$

$$g_2(\epsilon,\varphi)(\varrho) = \int_{-\infty}^{0} e^{2(\xi)} \frac{\varphi}{64} d\xi$$

$$\int_0^\epsilon Z_1(\epsilon,\xi,\varphi)(\varrho) d\xi = \int_0^\epsilon sin(\epsilon - \xi) \int_{-\infty}^{0} e^{2(\xi)} \frac{\varphi}{36} d\xi$$

$$\int_0^\epsilon Z_2(\epsilon,\xi,\varphi)(\varrho) d\xi = \int_0^\epsilon sin(\epsilon - \xi) \int_{-\infty}^{0} e^{2(\xi)} \frac{\varphi}{36} d\xi$$

To analyze the system defined in equations (4.1)-(4.3), we assume that the functions $\rho_i : [0,\infty) \to [0,\infty)$, for $i = 1,2$, are continuous. By applying these configurations, the system can then be rewritten in the theoretical form of the design given by equations (1.1)-(1.2). As a result, for $\epsilon \in [0,T]$ and $\varphi, \bar{\varphi} \in \mathcal{B}$, we obtain the following:

$$\begin{aligned} \|g_1(\epsilon,\varphi) - g_1(\epsilon,\bar{\varphi})\|_X &\leq \left(\int_0^\pi \left(\int_{-\infty}^{0} e^{2(\xi)} \left\| \frac{\varphi}{25} - \frac{\bar{\varphi}}{25} \right\| d\xi \right)^2 \right)^{\frac{1}{2}} \\ &\leq \left(\int_0^\pi \left(\frac{1}{25} \int_{-\infty}^{0} e^{2(\xi)} \sup \|\varphi - \bar{\varphi}\| d\xi \right)^2 \right)^{\frac{1}{2}} \end{aligned}$$

$$\begin{aligned} &\leq \frac{\sqrt{\pi}}{25}\|\varphi-\bar{\varphi}\|_{\mathcal{B}} \\ &\leq L_g\|\varphi-\bar{\varphi}\|_{\mathcal{B}}, \end{aligned}$$

$$\begin{aligned} \|g_2(\epsilon,\varphi)-g_2(\epsilon,\bar{\varphi})\|_X &\leq \left(\int_0^{\pi}\left(\int_{-\infty}^{0} e^{2(\xi)}\left\|\frac{\varphi}{16}-\frac{\bar{\varphi}}{16}\right\|d\xi\right)^2\right)^{\frac{1}{2}} \\ &\leq \left(\int_0^{\pi}\left(\frac{1}{16}\int_{-\infty}^{0} e^{2(\xi)}\sup\|\varphi-\bar{\varphi}\|d\xi\right)^2\right)^{\frac{1}{2}} \\ &\leq \frac{\sqrt{\pi}}{16}\|\varphi-\bar{\varphi}\|_{\mathcal{B}} \\ &\leq L_g\|\varphi-\bar{\varphi}\|_{\mathcal{B}}, \end{aligned}$$

$$\begin{aligned} \|Z_1(\epsilon,\xi,\varphi)-Z_1(\epsilon,\xi,\bar{\varphi})\|_X &\leq \left(\int_0^{\pi}\left(\int_{-\infty}^{0} e^{2(\xi)}\left\|\frac{\varphi}{36}-\frac{\bar{\varphi}}{36}\right\|d\xi\right)^2\right)^{\frac{1}{2}} \\ &\leq \left(\int_0^{\pi}\left(\frac{1}{36}\int_{-\infty}^{0} e^{2(\xi)}\sup\|\varphi-\bar{\varphi}\|d\xi\right)^2\right)^{\frac{1}{2}} \\ &\leq \frac{\sqrt{\pi}}{36}\|\varphi-\bar{\varphi}\|_{\mathcal{B}} \\ &\leq L_{Z_1}\|\varphi-\bar{\varphi}\|_{\mathcal{B}}. \end{aligned}$$

Similarly, we can deduce that

$$\begin{aligned} \|Z_2(\epsilon,\xi,\varphi)-Z_2(\epsilon,\xi,\bar{\varphi})\|_X &\leq \left(\int_0^{\pi}\left(\int_{-\infty}^{0} e^{2(\xi)}\left\|\frac{\varphi}{36}-\frac{\bar{\varphi}}{36}\right\|d\xi\right)^2\right)^{\frac{1}{2}} \\ &\leq \left(\int_0^{\pi}\left(\frac{1}{36}\int_{-\infty}^{0} e^{2(\xi)}\sup\|\varphi-\bar{\varphi}\|d\xi\right)^2\right)^{\frac{1}{2}} \\ &\leq \frac{\sqrt{\pi}}{36}\|\varphi-\bar{\varphi}\|_{\mathcal{B}} \\ &\leq L_{Z_2}\|\varphi-\bar{\varphi}\|_{\mathcal{B}}. \end{aligned}$$

Let $B : U \to X$ be defined by $Bu(\epsilon) = \mu(\epsilon,\varrho)$, for $0 \leq \varrho \leq \pi$, where $\mu : [0,T]\times[0,\pi] \to X$ is a continuous function.

Thus, the conditions (H1)-(H5) are satisfied. Furthermore, suppose the following values are assumed: $M = 1$, $e = 1$, $r^* = \frac{1}{2}$, $L^*_{g_1}, L^*_{g_2}, L^*_{Z_1}, L^*_{Z_2} = 0.3$, and $\eta = \frac{1}{2}$. In this case, we have the following calculation:

$$Me^{\eta}\left[L_{g_1}+\frac{L_{g_2}}{\Gamma(\eta+1)}+\frac{e(L_{Z_1}+L_{Z_2})}{(\eta+1)\Gamma(\eta)}\right]r^* = 0.04+\frac{1}{2}\left(\frac{0.6611}{0.8655}+\frac{2(0.053+0.22)}{3}\right)+\left(\frac{0.5}{0.8655}+\frac{2}{3}\right)$$

$$= 0.04+\frac{1}{2}(0.3154+0.2110)+0.6458+0.6888 = 0.7984 < 1.$$

Thus, by Theorem (3.1), we conclude that the system defined by equations (4.1)-(4.3) has a mild solution on the interval $[0,1]$.

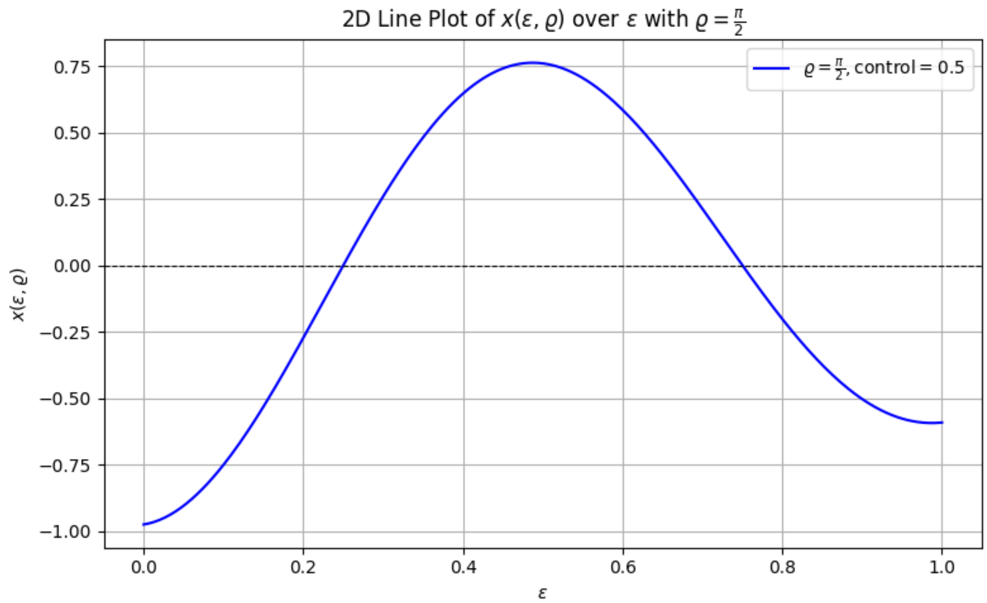

FIGURE 1. 2D Line Plot of $x(\epsilon, \varrho)$ over ϵ with $\varrho = \frac{\pi}{2}$ and control parameter control $= 0.5$

A 2D line plot in Figure 1 for the function $x(\epsilon, \varrho)$ describes the behavior of the object for a fixed parameter $\varrho = \frac{\pi}{2}$ in the time interval of $\epsilon \in [0, 1]$. The function is defined as $x(\epsilon, \varrho) = e^{-\text{control}\cdot\epsilon} \sin(\pi\varrho) \cos(2\pi\epsilon)$, with the control parameter causing damping. In this example, the control parameter is set to control $= 0.5$; this determines the rate at which the oscillatory amplitude decays with time. The plot is periodic because of the $\cos(2\pi\epsilon)$ term, which has a period of 1 unit. The oscillations are damped by the exponential decay factor $e^{-\text{control}\cdot\epsilon}$ and thus decay progressively as ϵ increases. When $\varrho = \frac{\pi}{2}$, the $\sin(\pi\varrho)$ term peaks at its maximum of 1, causing the oscillatory part to have the largest possible initial amplitude. There are also many zero crossings where the function changes sign; since the argument to the cosine function is periodic, these are also periodic. The control parameter would determine the damping rate; for a higher value, the decay of amplitude is faster, whereas for a smaller value, the oscillations could persist for longer. This animation depicts the effect of periodic oscillations and exponential damping together to provide insight into the behavior of damped oscillatory systems, like those found in mechanical vibrations, electrical circuits, and wave dynamics. The controlled decay ensures that the oscillations are gradually reduced, reflecting realistic scenarios where energy dissipation occurs over time.

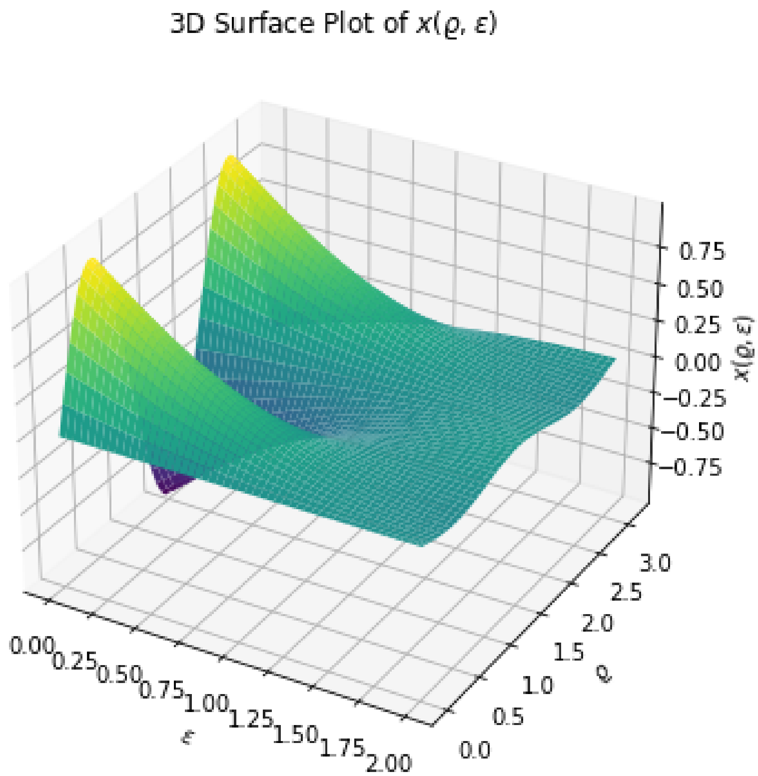

Figure 2. 3D Surface Plot of $x(\epsilon, \varrho)$ showing the variation of the function over $\epsilon \in [0, 2]$ and $\varrho \in [0, \pi]$.

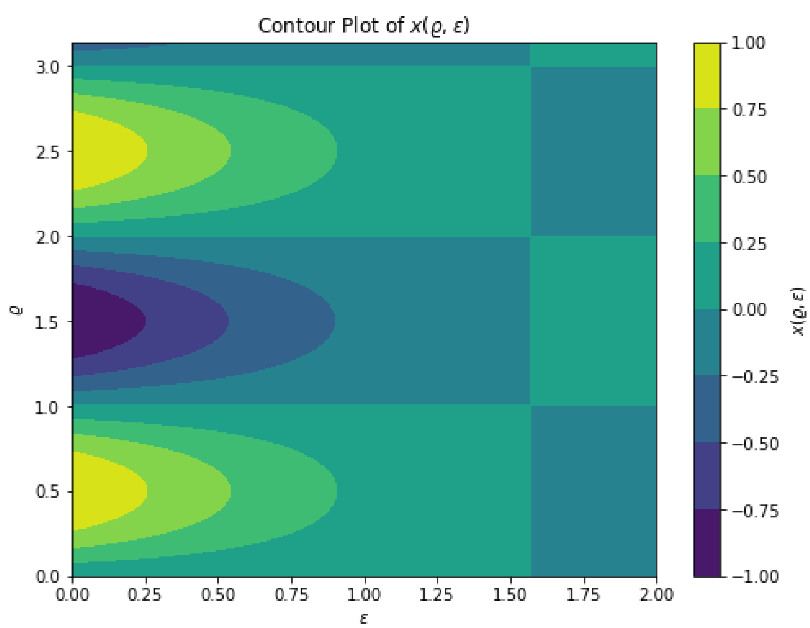

Figure 3. Contour Plot of $x(\epsilon, \varrho)$ over $\epsilon \in [0, 2]$ and $\varrho \in [0, \pi]$.

The graphical representations in Figures 2 and 3 provide a detailed visualization of the function $x(\epsilon, \varrho)$ over the parameter space defined by time ϵ and the oscillatory parameter ϱ. Figure 2 displays the 3D surface plot of the function $x(\epsilon, \varrho)$ over the time interval $\epsilon \in [0, 2]$ and for values of $\varrho \in [0, \pi]$. The function is given by $x(\epsilon, \varrho) = e^{-\epsilon} \sin(\pi\varrho) \cos(\epsilon)$. The surface plot captures the combined effects of two key components: the exponential decay factor $e^{-\epsilon}$ and the oscillatory behavior induced by the cosine term $\cos(\epsilon)$. Initially, at small values of ϵ, the amplitude of the function is relatively large due to the oscillations from the cosine term. However, since the exponential decay factor is an increasing function of ϵ, as ϵ gets larger, it makes the amplitude of the function reduce. The graph then becomes a flat surface at later values of ϵ, giving an idea about the damping as time progresses. The sine function, $\sin(\pi\varrho)$, affects the amplitude of the oscillation according to ϱ. When the value of ϱ is high, the oscillation increases. Therefore, the surface plot visually exhibits both the oscillatory nature of the solution and the damping effect as time progresses. The resulting surface thus shows how oscillations gradually decline with time while remaining modulated by the value of ϱ.

Figure 3 depicts the contour plot of the same function $x(\epsilon, \varrho)$ over the ϵ-ϱ plane. In this plot, each contour line represents a constant value of $x(\epsilon, \varrho)$, with the spacing between the contours indicating the rate of change of the function with respect to both ϵ and ϱ. The color gradient in the contour plot is used to visually represent the magnitude of $x(\epsilon, \varrho)$, with different colors corresponding to different values of the function. Just like in the case of the contour plot, the oscillation nature from the function $x(\epsilon, \varrho)$ is presented in the contour plot. The contours separate with time ϵ, which means that the oscillation amplitudes are decaying due to the exponential factor $e^{-\epsilon}$. This decaying process is easily noticed in the contour plot since their distance is increasing with time. On the other hand, for higher values of ϱ, the contours are closer together and so oscillation is stronger. This behavior can be understood from the sine term $\sin(\pi\varrho)$ in terms of amplitudes of oscillations by ϱ. Thus, the contour plot gives a 2-dimensional view of the behavior shown at the surface in the 3D plot. Although the surface plot is more vivid by capturing the dynamics in three dimensions, the contour plot allows a better understanding of the spatial distribution of the values of $x(\epsilon, \varrho)$ in terms of ϵ and ϱ.

Both the 3D surface plot and the contour plot give an overall visualization of how $x(\epsilon, \varrho)$ changes in time and how it is being controlled by the modulation parameter ϱ. Damping effect, which appears in the form of an exponential term, $e^{-\epsilon}$, reduces the amplitude as time increases. The oscillations themselves are damped by the cosine term $\cos(\epsilon)$ and the sine term $\sin(\pi\varrho)$, the latter of which depends on the amplitude of the oscillations according to the value assigned to ϱ. These plots become very useful to examine systems oscillatory and decaying with time simultaneously, say in mechanical circuits, electrical circuits, or in wave propagation phenomena. The results show that the behavior of the system is strongly influenced by the presence of time and the oscillatory parameter ϱ, revealing valuable information concerning the temporal evolution and parameter sensitivity of such a system.

5. Application to Cryptography: Secure Key Generation Framework

In this section, we consider some possible cryptographic applications of the system stated by fractional neutral VFIDEs with SDD (Equations (1.1) and (1.2)). The properties of chaos and unpredictability of the system along with the sensitivity to initial conditions and control parameters make it a prime candidate for applications to secure cryptography. This would guarantee that the produced keys are securely random and have a suitable unpredictability to ensure them adequate for modern encryption schemes like symmetric encryption and public-key cryptography. Public-key cryptography gets its justification in terms of key generation, which has to be generated in a sufficiently random and nondeterministic manner.

5.1. **Key Characteristics Supporting Cryptographic Applications.** A key feature of this system is a chaotic component due to the presence of fractional-order derivatives and SDDs. Specifically, the model in the problem is governed by the fractional neutral VFIDE with SDDs, where the terms g_1, g_2, Z_1, and Z_2 have played the crucial role in the behavior of the system. The term g_1 introduces memory effects and is responsible for the sensitivity of the system to initial conditions, since a very small variation in the initial state Z_1 or in the control parameters can result in radically different outputs, thus giving strong properties to keys generated in such a system.

Similarly, the symbol g_2, which incorporates the nonlinear dynamics of the system, enhances the chaotic behavior and ensures that the evolution of the system is complex and cannot be reverse-engineered. This nonlinearity is important for cryptographic applications because it makes the system resistant to attacks in which an adversary tries to deduce the key by analyzing known system behavior or partial knowledge of previous outputs. The two terms, Z_1 and Z_2, refer to different states or parameters influencing the evolution of the system at different times. In this, the interchange of these terms with each other, through the SDDs, ensures a very nonlinear and chaotic manner of evolution of the system. The dependence on Z_1 and Z_2 guarantees that even the smallest change in these states results in a completely different trajectory for the system. This sensitivity makes it practically impossible for an attacker to predict future keys based on previous outputs, thus giving strong resistance against key prediction or cryptanalysis. Therefore, the mixing of these words-g_1, g_2, Z_1, and Z_2-makes the keys, generated by this system, both unpredictable and quite complex, offering protection against both brute-force attacks and reverse engineering.

5.2. **Cryptographic Key Generation Mechanism.** The role of the system in the key generation can be described as follows: given a set of initial conditions, say, an initial seed for the key, the system evolves with time according to the integro-differential equations, whose terms g_1, g_2, Z_1, and Z_2 contribute to the output, which represents the cryptographic key, $\varrho(\epsilon)$. These terms lead to chaotic behavior, so the produced keys are as unpredictable as possible, and they resist attacks. This framework is ideal for cryptographic systems to resist external attacks on key generation in the sense that keys produced here are hard to duplicate or anticipate by unauthorized parties. The unique feature in the system, such as sensitivity to initial conditions, chaotic patterns, and nonlinearity, will result in the production of a completely different set of cryptographic keys whenever the system is initialized. In other words, the keys produced will be virtually random and resistant to cryptanalysis.

Moreover, the output of the system may be used as a cryptographic key or may undergo further processing (such as hashing) to be usable with more typical cryptographic algorithms such as AES or RSA. Chaotic dynamics, controlled by the terms g_1, g_2, Z_1, and Z_2, guarantee that the keys generated differ from all of their predecessors; thus, making it virtually impossible for an attacker to predict further keys or reverse-engineer any part of the key sequence knowing some portion of the past values.

5.3. **Graphical Representation of System Behavior.** We also present a set of graphical representations to understand the dynamic nature of the system and its suitability for cryptographic applications. This includes 2D, 3D, and contour plots representing the system behavior in different domains. The following figures depict chaotic dynamics of the system and the consequences in the context of secure key generation.

5.3.1. *Dynamic Evolution of $\varrho(\epsilon)$.* Figure 4 displays the dynamic evolution of $\varrho(\epsilon)$ for different initial conditions and control parameters. In this 2D plot, the system is sensitive to its initial conditions. This is the most important characteristic of a chaotic system in terms of cryptography: the plot displays how small differences in initial conditions or control parameters lead to qualitatively very different evolutions over time. This feature is critical for the generation of cryptographic keys, ensuring that the keys produced by the system are unique and unpredictable. The sensitivity of the system makes it nearly impossible to reverse-engineer or predict future key values, which provides a good defense against attacks that are based on predicting the keys or recovering them from previous values. Exploiting this chaotic nature, the system guarantees that no two keys will be alike, even if the initial conditions are similar.

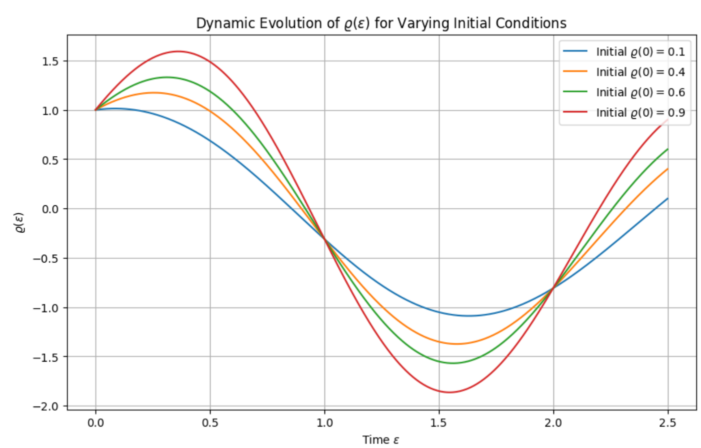

FIGURE 4. Dynamic evolution of $\varrho(\epsilon)$ under varying initial conditions and control parameters. The trajectories demonstrate the sensitivity and chaotic behavior of the system, critical for secure cryptographic key generation.

5.3.2. *Solution Space Complexity.* Figure 5 shows a 3D surface plot of $\varrho(\epsilon)$ versus time ϵ and parameter ϱ. This plot visualizes the solution space complexity of the system. The surface contains complex patterns, which underpin the chaotic and nonlinear nature of the system; this is also the reason behind the randomness and unpredictability of the output. The complexity of the solution space will ensure that keys generated for encryption and decryption operations are non-predictive to the greatest extent. Surface plots of the fluctuations show highly nonlinear behavior where the system cannot evolve in any predictable manner and therefore is suitable for cryptographic use when strong randomness is required, like in highly secure applications. The behavior of the system, as shown in this plot, ensures that keys produced by the system are highly resistant to reverse engineering or attacks based on previously generated keys.

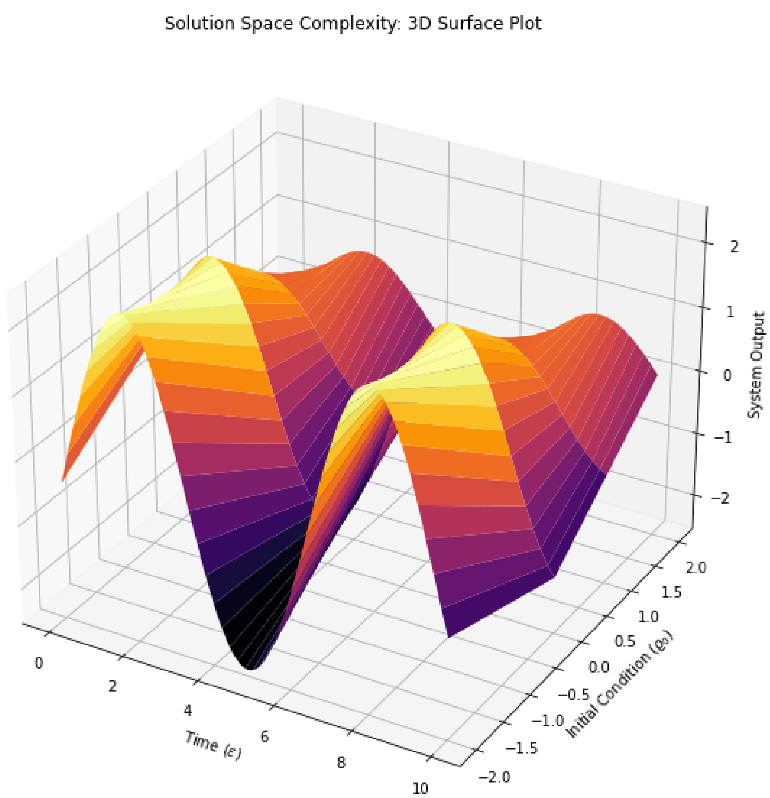

Figure 5. 3D surface plot showing the dynamic evolution of $\varrho(\epsilon)$ over time ϵ and parameter ϱ. The complex, nonlinear fluctuations highlight the chaotic nature of the system, critical for cryptographic security.

5.3.3. *Chaotic Patterns in Contour Representation.* Figure 6 is a contour plot of the behavior of $\varrho(\epsilon)$ with respect to time ϵ and parameter ϱ. The pattern in the plot is highly irregular and complex, which is typical of chaotic systems. These unpredictable patterns strengthen the case for the system's use in cryptographic key generation, since the keys produced will be highly random and secure. The non-repetitive nature of the contour plot shows that the system's behavior is not predictable or periodic, which is a must for key generation systems that are to be resistant to cryptanalysis. The chaotic behavior of the system ensures that the keys remain unpredictable and cannot be replicated even if past keys are known. This is one of the essential features of modern cryptography, which has security based on the unpredictability of future keys or even deriving them from earlier keys.

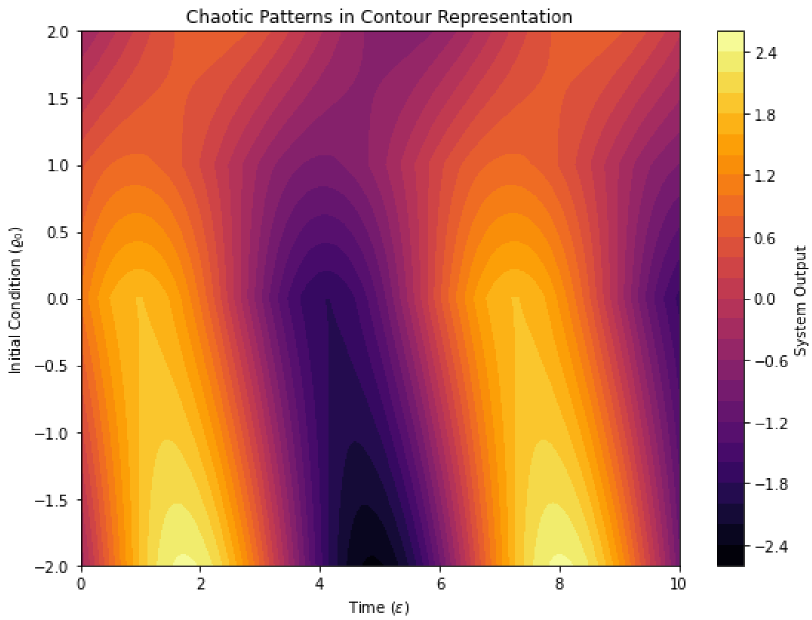

FIGURE 6. Contour plot of $\varrho(\epsilon)$ over the ϵ-ϱ domain, showing the complex, unpredictable patterns that reinforce the system's suitability for generating highly secure cryptographic keys.

The graphical representations above-2D, 3D, and contour plots-represent the sensitive dependence on initial conditions, complexity of the solution space, and chaotic behavior of the system. These are the characteristics that the generation of unpredictable cryptographic keys needs. The dynamic evolution of $\varrho(\epsilon)$ ensures that the keys generated are unique and not susceptible to attacks such as brute-force and reverse-engineering. The system is inherently chaotic, and that guarantees no two keys will ever be alike, providing a robust framework for secure key generation in cryptographic applications. The system of fractional neutral VFIDE with SDD is mathematically rich and powerful for generating secure keys. By utilizing the sensitivity, controllability, and chaos nature of the system, we can generate keys that are unique and unpredictable, thus resisting cryptographic attacks. Graphical representations further validate the system's potential as a robust tool for advanced cryptographic frameworks, to ensure security in applications requiring such a high level of confidentiality and integrity.

6. Conclusion

In this paper, we perform a comprehensive study of the state-dependent fractional neutral VFIDE, with the Caputo fractional derivative being used to describe fractional differentiation. We use Schauder's fixed point theorem to establish some controllability results under specific conditions. We then provide a detailed example to validate our theoretical findings and perform numerical simulations, showing the convergence of the actual solution in the dynamic evolution of the system. Graphical analysis further clarifies the behavior of the solution under various conditions and highlights the sensitivity of the system to initial conditions and parameters. This work further explores potential applications of these equations in cryptography, as the system's chaotic nature, due to fractional-order derivatives and SDDs, especially makes it apt for secure key generation. The unpredictability and sensitivity of chaotic systems to initial conditions will ensure that the produced cryptographic keys are complex, random, and resist cryptanalytic attacks. Therefore, the play of terms involving g_1, g_2, Z_1, and Z_2 leads to the generation of secure keys that are not predictable, showing the applicability of this system in advanced cryptographic applications. Hence, both controllability analysis and cryptographic applications conclude the flexibility of fractional neutral VFIDE with SDD. New directions in the form of practical applications in various domains can now be envisaged from these findings, particularly those which are highly critical of real-world models in the requirement of security with the occurrence of complex dynamic behavior.

Acknowledgement: The authors A. Aloqaily and N. Mlaiki would like to thank Prince Sultan University for paying the APC and for the support through the TAS research lab.

Conflicts of Interest: The authors declare that there are no conflicts of interest regarding the publication of this paper.

References

[1] T. Abdeljawad, A Lyapunov Type Inequality for Fractional Operators with Nonsingular Mittag-Leffler Kernel, J. Inequal. Appl. 2017 (2017), 130. https://doi.org/10.1186/s13660-017-1400-5.

[2] T. Abdeljawad, D. Baleanu, Discrete Fractional Differences with Nonsingular Discrete Mittag-Leffler Kernels, Adv. Differ. Equ. 2016 (2016), 232. https://doi.org/10.1186/s13662-016-0949-5.

[3] T. Abdeljawad, D. Baleanu, On Fractional Derivatives with Exponential Kernel and Their Discrete Versions, Rep. Math. Phys. 80 (2017), 11–27. https://doi.org/10.1016/s0034-4877(17)30059-9.

[4] Y. Zhou, Basic Theory of Fractional Differential Equations, World Scientific, Singapore, 2014. https://doi.org/10.1142/13289.

[5] A.A. Kilbas, H.M. Srivastava, J.J. Trujillo, Theory and Applications of Fractional Differential Equations, Elsevier, Amsterdam, 2006. https://doi.org/10.1016/s0304-0208(06)x8001-5.

[6] R.P. Agarwal, B. de Andrade, G. Siracusa, On Fractional Integro-Differential Equations with State-Dependent Delay, Comput. Math. Appl. 62 (2011), 1143–1149. https://doi.org/10.1016/j.camwa.2011.02.033.

[7] M. Benchohra, F. Berhoun, Impulsive Fractional Differential Equations With State-Dependent Delay, Commun. Appl. Anal. 14 (2010), 213–224.

[8] T. Guendouzi, L. Bousmaha, Approximate Controllability of Fractional Neutral Stochastic Functional Integro-Differential Inclusions with Infinite Delay, Qual. Theory Dyn. Syst. 13 (2014), 89–119. https://doi.org/10.1007/s12346-014-0107-y.

[9] Z. Liu, M. Bin, Approximate Controllability for Impulsive Riemann-Liouville Fractional Differential Inclusions, Abstr. Appl. Anal. 2013 (2013), 639492. https://doi.org/10.1155/2013/639492.

[10] P. Balasubramaniam, P. Tamilalagan, Approximate Controllability of a Class of Fractional Neutral Stochastic Integro-Differential Inclusions with Infinite Delay by Using Mainardi's Function, Appl. Math. Comput. 256 (2015), 232–246. https://doi.org/10.1016/j.amc.2015.01.035.

[11] I. Podlubny, Fractional Differential Equations, Academic Press, New York, 1999.

[12] F. Mainardi, P. Paradisi, R. Gorenflo, Probability Distributions Generated by Fractional Diffusion Equations, in: J. Kertesz, I. Kondor (Eds.), Econo-physics: An Emerging Science, Kluwer Academic, Dordrecht, 2000.

[13] T. Gunasekar, P. Raghavendran, S.S. Santra, M. Sajid, Existence and Controllability Results for Neutral Fractional Volterra-Fredholm Integro-Differential Equations, J. Math. Comput. Sci. 34 (2024), 361–380. https://doi.org/10.22436/jmcs.034.04.04.

[14] P. Raghavendran, T. Gunasekar, S.S. Santra, D. Baleanu, D. Majumder, Analytical Study of Existence, Uniqueness, and Stability in Impulsive Neutral Fractional Volterra-Fredholm Equations, J. Math. Comput. Sci. 38 (2024), 313–329. https://doi.org/10.22436/jmcs.038.03.03.

[15] A. Hamoud, Existence and Uniqueness of Solutions for Fractional Neutral Volterra-Fredholm Integro Differential Equations, Adv. Theory Nonlinear Anal. Appl. 4 (2020), 321–331. https://doi.org/10.31197/atnaa.799854.

[16] A. Hamoud, N. Mohammed, K. Ghadle, Existence and Uniqueness Results for Volterra-Fredholm Integro Differential Equations, Adv. Theory Nonlinear Anal. Appl. 4 (2020), 361–372. https://doi.org/10.31197/atnaa.703984.

[17] P. Raghavendran, T. Gunasekar, D. Baleanu, S.S. Santra, D. Majumder, Neural Network Framework for Controllability of Fractional Volterra Fredholm Integro-Differential Equations with State-Dependent Delay, J. Math. Comput. Sci. 40 (2025), 292–309. https://doi.org/10.22436/jmcs.040.03.01.

[18] A. Columbu, S. Frassu, G. Viglialoro, Refined Criteria Toward Boundedness in an Attraction–repulsion Chemotaxis System with Nonlinear Productions, Appl. Anal. 103 (2023), 415–431. https://doi.org/10.1080/00036811.2023.2187789.

[19] A. Hamoud, K. Ghadle, Some New Uniqueness Results of Solutions for Fractional Volterra-Fredholm Integro-Differential Equations, Iran. J. Math. Sci. Inform. 17 (2022), 135–144. https://doi.org/10.52547/ijmsi.17.1.135.

[20] A. Ndiaye, F. Mansal, Existence and Uniqueness Results of Volterra–Fredholm Integro-Differential Equations via Caputo Fractional Derivative, J. Math. 2021 (2021), 5623388. https://doi.org/10.1155/2021/5623388.

[21] Z. Dahmani, New Existence and Uniqueness Results for High Dimensional Fractional Differential Systems, Facta Univ. Ser.: Math. Inform. 30 (2015), 281–293.

[22] H. HamaRashid, H.M. Srivastava, M. Hama, P.O. Mohammed, E. Al-Sarairah, M.Y. Almusawa, New Numerical Results on Existence of Volterra–Fredholm Integral Equation of Nonlinear Boundary Integro-Differential Type, Symmetry 15 (2023), 1144. https://doi.org/10.3390/sym15061144.

[23] P. Kalamani, D. Baleanu, S. Selvarasu, M. Mallika Arjunan, On Existence Results for Impulsive Fractional Neutral Stochastic Integro-Differential Equations with Nonlocal and State-Dependent Delay Conditions, Adv. Differ. Equ. 2016 (2016), 163. https://doi.org/10.1186/s13662-016-0885-4.

[24] E. Hernández, A. Prokopczyk, L. Ladeira, A Note on Partial Functional Differential Equations with State-Dependent Delay, Nonlinear Anal.: Real World Appl. 7 (2006), 510–519. https://doi.org/10.1016/j.nonrwa.2005.03.014.

[25] P. Raghavendran, T. Gunasekar, J. Ahmad, W. Emam, A Study on the Existence, Uniqueness, and Stability of Fractional Neutral Volterra-Fredholm Integro-Differential Equations with State-Dependent Delay, Fractal Fract. 9 (2024), 20. https://doi.org/10.3390/fractalfract9010020.